Unraveling the Ground State and Excited State Structures and Dynamics of Hydrated Ce3+ Ions by Experiment and Theory

Patric Lindqvist-Reis, Florent Réal, Rafal Janicki, Valérie Vallet

Inorganic Chemistry
Cite This: Inorg. Chem. 2018, 57, 10111−10121
Article
pubs.acs.org/IC

Unraveling the Ground State and Excited State Structures and Dynamics of Hydrated Ce^{3+} Ions by Experiment and Theory

Patric Lindqvist-Reis,*[,†] Florent Réal,*[,‡] Rafał Janicki,[∥] and Valérie Vallet*[,‡]

[†]Institute for Nuclear Waste Disposal, Karlsruhe Institute of Technology, P.O. Box 3640, 76021 Karlsruhe, Germany
[‡]University of Lille, CNRS, UMR 8523 - PhLAM - Physique des Lasers Atomes et Molécules, F-59000 Lille, France
[∥]University of Wrocław, Faculty of Chemistry, F. Joliot-Curie 14, 50-383 Wrocław, Poland

Supporting Information

ABSTRACT: The 4f-5d transition of Ce^{3+} provides favorable optical spectroscopic properties such as high sensitivity and quantum yield, making it a most important dopant for lanthanide-activated phosphors. A key for the design of these materials with fine-tuned color emission is a fundamental understanding of the Ce^{3+} ground state and excited state structures and the dynamics of energy transfer. Such data is also crucial for deriving coordination chemistry information on Ce^{3+} ions in different chemical environments directly from their optical spectra. Here, by combining 4f-5d absorption and luminescence spectroscopy and highly accurate quantum chemical electronic structure calculations, we study the interplay between the local structure of Ce^{3+} in aqueous solutions and in crystalline hydrates, the strengths of Ce−O/Cl interactions with aqua and chloride ligands, and the resulting absorption and luminescence spectra. Experimental and theoretical absorption spectra of $[Ce(H_2O)_9]^{3+}$ and $[Ce(H_2O)_8]^{3+}$ with defined geometries provide a means for analyzing the equilibrium between these species in aqueous solution as a function of temperature ($K(298) = 0.20 \pm 0.03$), while analyses of spectra of different aqua-chloro complexes reveal that eight-coordinate aqua-chloro complexes are present in solution at high chloride concentration. An intriguing feature in these systems concerns the large observed Stokes shifts, 5500−10 100 cm^{-1}. By exploring the excited state potential energy surfaces with relativistic multireference calculations, we show that these shifts result from significant geometrical relaxation processes in the lowest $5d^1$ excited state. For $[*Ce(H_2O)_8]^{3+}$ the relaxation gives shorter Ce−O bonds and a Stokes shift of ∼5500 cm^{-1}, while for $[*Ce(H_2O)_9]^{3+}$ the lowest $5d^1$ state results in a spontaneous dissociation of a water molecule and a Stokes shift of ∼10 100 cm^{-1}. These findings are important for the understanding and optimization of luminescence properties of cerium complexes.

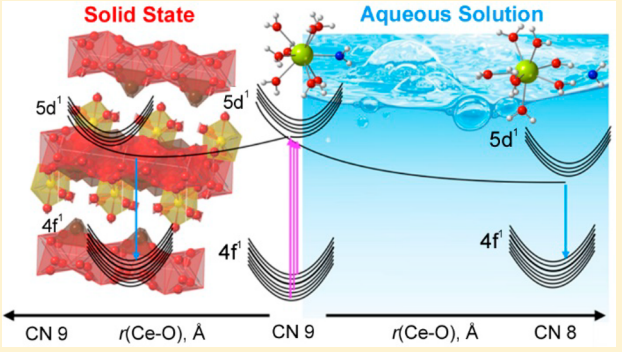

INTRODUCTION

Speciation of lanthanide (Ln) and actinide (An) ions in aqueous systems is of utmost importance for the design and development of selective extraction agents for the separation of Ln^{3+} and An^{3+} ions for partitioning and transmutation. Stoichiometry and coordination geometry data of complexes of these ions and thermodynamic stability data are essential for the prediction of actinide migration in natural aquifers around a nuclear waste repository.[1] Various spectroscopic and scattering techniques may be used to probe the chemical and coordination structures of lanthanide and actinides ions in aqueous solution.[2,3] While synchrotron-based X-ray absorption fine structure (XAFS) spectroscopy provides accurate metal−oxygen distances, the number of water molecules residing in the first hydration shell—the hydration number—cannot typically be obtained with an accuracy better than about 10%.[4] This is a drawback for determining hydration numbers of Ln^{3+} and An^{3+} ions in aqueous solution. Moreover, owing to the core-hole lifetime of the lanthanide and actinide K and L_3 absorption edges, the corresponding X-ray absorption near-edge structures (XANES) of the aqueous Ln^{3+} and An^{3+} ions are relatively unaffected by the coordination geometry.[5] Thus, the question of whether these ions are eight- or nine-coordinate is difficult to answer with X-ray absorption spectroscopies. UV−vis and fluorescence spectroscopy can also be used to gain insight on the Ln/An coordination sphere.[6] For lanthanide ions like Eu^{3+} and Tb^{3+} and for the actinide ions Am^{3+} and Cm^{3+}, atom-like absorption and luminescence bands are due to parity forbidden 4f-4f and 5f-5f transitions, respectively. However, for Ce^{3+}, parity-allowed 4f-5d transitions give rise to broad absorption and luminescence bands in the ultraviolet and short (nanoseconds) luminescence lifetimes. Its total ligand-field splitting of the $^{2S+1}L_J$ states of the $4f^1$ configuration is much smaller than the total splitting of the five 5d orbitals. The energy gap between the barycenters of these configurations is ∼40 000 cm^{-1} for the aqueous $[Ce(H_2O)_9]^{3+}$ ion.[7] In addition to a special redox capability

Received: May 9, 2018
Published: August 9, 2018

DOI: 10.1021/acs.inorgchem.8b01224
Inorg. Chem. 2018, 57, 10111−10121

between the IV and III states induced by photoabsorption, which has been utilized in molecular photoemitting compounds,[8a−d] the 4f-5d transition offers favorable optical spectroscopic properties such as high sensitivity and quantum yield, making Ce^{3+} a most important dopant for lanthanide-activated phosphors.[8e]

In this work we address the question of whether there is a relationship between the 4f-5d absorption and luminescence spectra and the coordination structure of Ce^{3+}. In dilute aqueous solutions the Ce^{3+} ion is expected to coordinate 9 water molecules in a first hydration shell and about 18 water molecules in a less well-defined second hydration shell.[4] A key confirmation that $[Ce(H_2O)_9]^{3+}$ is the predominant species in aqueous solution is the marked similarity between its 4f-5d absorption spectrum and that of Ce^{3+} in $[La(H_2O)_9](C_2H_5SO_4)_3$, both of which give rise to five broad bands between 200 and 255 nm.[9−12] The solution spectrum also contains a weak sixth band at 295 nm that has been attributed to the admixture of transitions to the lowest 5d energy level of a minor $[Ce(H_2O)_8]^{3+}$ species.[9−14] This band gains intensity with increasing temperature and reduces intensity with increasing pressure,[11−13,15] indicating that octa- and nona-aqua cerium species are in equilibrium controlled by temperature and pressure (eq 1).

$$[Ce(H_2O)_9]^{3+} \rightleftharpoons [Ce(H_2O)_8]^{3+} + H_2O \quad (1)$$

Although this is a rational model the existence of an octahydrate species in solution has not been proven spectroscopically. Most hydration models on trivalent lanthanide and actinide ions in aqueous solution comprise octa- and nona-aqua equilibrium species, and for the lanthanides it is known that the water exchange rate of octa- and nona-hydrate ions is highest in the middle of the series.[16] However, only a few experimental studies have provided thermodynamic quantities for trivalent lanthanide and actinide ions of the equilibrium eq 1.[6a,12,15]

The preliminary assignment of the UV-absorption spectrum of the $Ce^{3+}(aq)$ ion was supported by electrostatic point charge and dipole moment model calculations, angular overlap model calculations, and INDO/S−CI calculations.[17] These calculations showed that the energy spacing between the 5d excited Kramer doublets varies significantly with the local structure and that the lowest 5d doublet of $[Ce(H_2O)_8]^{3+}$ for a range of different coordination polyhedra is at lower energy than the lowest component of $[Ce(H_2O)_9]^{3+}$ in tricapped trigonal prismatic geometry.[17] This suggests that it is feasible to derive information about the coordination geometry, and thus the hydration number, of the Ce^{3+} equilibrium species in aqueous solution directly from the UV−vis absorption spectrum.

Kaizu et al.[11] studied the decay and rise transients in the excited $5d^1$ state of $[*Ce(H_2O)_9]^{3+}$ (* denotes a photoexcited species) in aqueous solution and suggested that it undergoes a fast dissociation of a first-shell water molecule to give rise to an octahydrate species, $[*Ce(H_2O)_9]^{3+} \rightarrow [*Ce(H_2O)_8]^{3+} + H_2O$. This is not an equilibrium reaction as of eq 1: it describes a photoinduced dissociation of water ligand from the nona-aqua species in the excited state. This is reflected in the extremely short luminescence lifetime of the nona-aqua species compared to the octaaqua species, 0.43 and 48 ns, respectively.[11] Thus, a steady state luminescence spectrum of a dilute aqueous Ce^{3+} solution monitors almost exclusively the $[*Ce(H_2O)_8]^{3+}$ species, which appears as a broad, unresolved doublet at 350 nm.[11−13] In comparison, the position of the luminescence band of $[*Ce(H_2O)_9]^{3+}$ in $[La(H_2O)_9](C_2H_5SO_4)_3$ is at 330 nm.[10]

In this paper we study comprehensively the course of the hydration equilibrium of eq 1 by combining complementary experimental and theoretical data. An important aim is to ascertain how the local structure of hydrated Ce^{3+} ions in nine- and eight-coordination is reflected in their respective absorption and luminescence spectra. Another objective is to study the ground state and the excited state structure and dynamics of the hydrated Ce^{3+} ion in solution. We first study how different coordination geometries and stoichiometries of six model compounds comprising $[Ce(H_2O)_9]^{3+}$, $[Ce(H_2O)_7Cl_2]^{+}$, $[Ce(H_2O)_8]^{3+}$, $[Ce(H_2O)_7Cl]^{2+}$, and $[Ce(H_2O)_6Cl_2]^{+}$ complexes with known crystal structures are reflected in the 4f-5d absorption and luminescence spectra. The absorption spectra of the nona- and octahydrates are used to elucidate the coordination modes of the hydrated Ce^{3+} ion in aqueous solution at ambient and elevated temperatures, which is necessary for deriving thermodynamic quantities of the equilibrium of eq 1, while the spectra of the mixed aqua-chloro species serve as references for solution spectra subject to Ce−Cl contact ion pair formation (inner-sphere complexes) in chloride background electrolytes.

The second part of the paper presents results of highly accurate quantum chemical electronic structure calculations on cerium complexes mimicking those in the model compounds. These calculations extend the previous work of Kotzian et al. on Ce^{3+} aqua ions,[17] by examining in detail the nature of the Ce−O and Ce−Cl chemical bonds using the method of quantum theory of atoms in molecules, and how these bonds together with the coordination environment influence the ligand field of the Ce^{3+} 5d orbitals, which has substantial impact on the absorption and luminescence spectra. A theoretical value of the Gibbs free energy of the hydration equilibrium eq 1 is presented and compared with the experimental value. Finally, these quantum chemical calculations will be used to explore for the first time the potential energy landscape of the photoexcited $[*Ce(H_2O)_9]^{3+}$ and $[*Ce(H_2O_7)Cl_2]^{+}$ ions, mapping precisely the photodissociative reaction path of an aqua ligand leaving the coordination sphere of these species and thus providing evidence for the photodissociative character of the lowest $5d^1$ excited state and the origin of the large Stokes shifts observed for the hydrated Ce^{3+} ions in dilute aqueous solution and in chloride electrolyte solutions. In order to properly compare the experimental and computed Stokes shifts, we define the latter as the energy difference between centroids of the lowest (Ce^{3+}) $5d^1$ level and the $^2F_{5/2}$ state.[18]

RESULTS AND DISCUSSION

Crystal Structures of Model Compounds. Figure 1 shows the coordination geometries of the host metal ion complexes in $[La(H_2O)_9](BrO_3)]_3$ (**1**), $[La(H_2O)_9](CF_3SO_3)_3$ (**2**), $([La(H_2O)_7Cl_2])_2Cl_2$ (**3**), $[Y(H_2O)_8]Cl_3\cdot$15-crown-5 (**4**), $[Ce(H_2O)_7Cl]Cl_2\cdot$15-crown-5$\cdot H_2O$ (**5**), and $[Y(H_2O)_6Cl_2]Cl$ (**6**).[19a−e] Further structure details are provided in Figure S1 and Tables S1−S4 in the Supporting Information. The coordination geometry of $[La(H_2O)_9]^{3+}$ in **1** and **2** is a tricapped trigonal prism with D_{3h} and C_{3h} point symmetries,[19a,b] respectively, while the dimeric $[(La(H_2O)_7Cl_2)_2]^{2+}$ species in **3** has a distorted tricapped trigonal prismatic coordination geometry.[19c] The $[Y(H_2O)_8]^{3+}$ and $[Ce(H_2O)_7Cl]^{2+}$ cations in **4** and **5** have distorted bicapped

DOI: 10.1021/acs.inorgchem.8b01224
Inorg. Chem. 2018, 57, 10111−10121

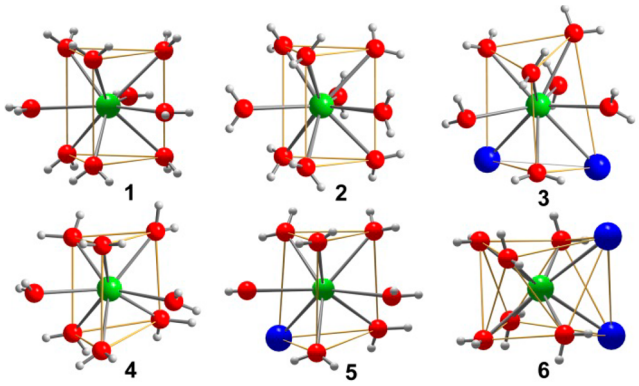

Figure 1. Coordination structures of the host metal ions in **1**–**6**. The coordination structures of the doped Ce^{3+} ions are expected to be similar to those of the host. The oxygen and chloride atoms of the principal coordination figures are connected.

trigonal prismatic geometries,[19d] while $[Y(H_2O)_6Cl_2]^+$ in **6** has a distorted square antiprismatic geometry.[19e] The coordination geometries of the doped Ce^{3+} ions are similar to those of the host metal ions, but due to the difference in ionic radii[20] between Ce^{3+} and the host metal ions the mean Ce–O bond distances are estimated to be ∼0.02 Å shorter than the mean La–O distances in **1**–**3** and ∼0.13 Å longer than the mean Y–O distances in **4** and **6** (Table S1). **5** is a "neat" compound where the cations are exclusively $[Ce(H_2O)_7Cl]^{2+}$ (Figure S1). It is interesting to note that the hydrated complex in **5** has a different structure and stoichiometry than those in the isotypic series $[M(H_2O)_9]Cl_3{\cdot}H_2O{\cdot}$15-crown-5 (M = La, Nd) and $[M(H_2O)_8]Cl_3{\cdot}$15-crown-5 (M = Nd–Lu).[6c,21a,b]

Absorption and Luminescence Spectra of $[Ce(H_2O)_9]^{3+}$ and $[Ce(H_2O)_8]^{3+}$. Figure 2 shows the 4f-5d absorption and luminescence spectra of $[Ce(H_2O)_9]^{3+}$ (**1**, **2**) and $[Ce(H_2O)_8]^{3+}$ (**4**) together with the spectra of the hydrated Ce^{3+} ion in aqueous solution at room temperature. The absorption spectra are confined between 200 and 300 nm. No absorption bands from water is expected in this region. Thus, the spectra are assigned to electronic transitions from the $^2F_{5/2}$ ground state to the two $^2D_{3/2}$ and three $^2D_{5/2}$ levels of the excited state. The spectra of $[Ce(H_2O)_9]^{3+}$ in **1** and **2** are similar with five characteristic absorption bands in the region 200–255 nm, showing that the Ce^{3+} ions in these compounds have similar symmetry and crystal field strength. No bands are observed above 255 nm, in accord with the absorption spectrum of Ce^{3+} in solid $[La(H_2O)_9](C_2H_5SO_4)_3$.[9−12] In contrast, the absorption spectrum of $[Ce(H_2O)_8]^{3+}$ in **4** differs markedly from those of $[Ce(H_2O)_9]^{3+}$ in **1** and **2**. The most striking difference is the position of the high wavelength band at 290 nm in **4** compared to 250–255 nm in **1** and **2**. In all the spectra the absorption bands are broadened by vibronic contributions. Even at 4 K the zero-phonon and vibronic lines are not resolved in **2** and **4** (Figure S2).

The absorption spectra of the hydrated Ce^{3+} ion in aqueous solution and in **2** are very similar, clearly indicating that the predominant species in solution has a tricapped trigonal prismatic coordination geometry. The spectrum of $[Ce(H_2O)_9]^{3+}$ in **2** is almost identical to that in $[La(H_2O)_9](C_2H_5SO_4)_3$.[9−12] This is rational as the coordination geometry of the lanthanide ions in the two compounds is essentially the same. One important difference between the spectra of the aqueous solution and **1** and **2** is the weak band at ∼296 nm

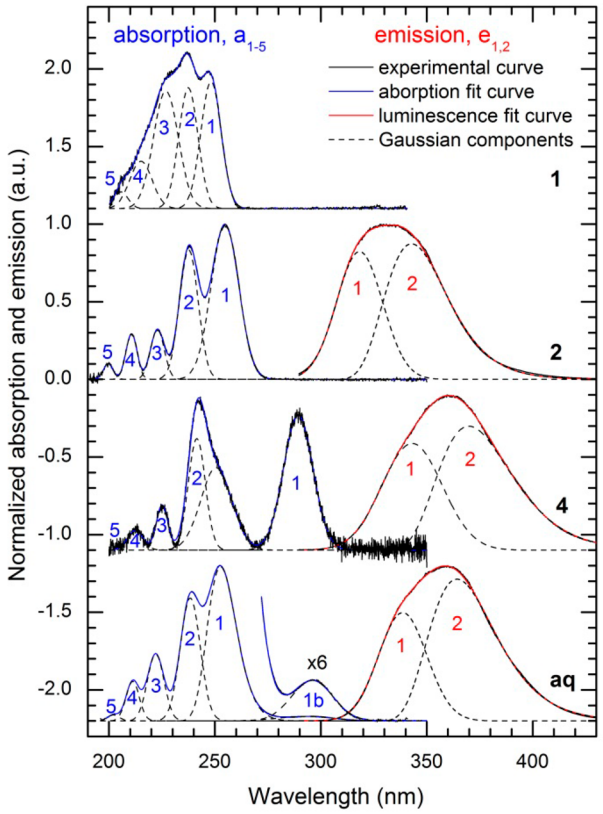

Figure 2. Comparison of the 4f-5d absorption and luminescence spectra of $[Ce(H_2O)_9]^{3+}$ (**1**, **2**), $[Ce(H_2O)_8]^{3+}$ (**4**), and Ce^{3+} in dilute aqueous solution (**aq**, 1.3 mM $Ce(ClO_4)_3$ in 10 mM $HClO_4$) at room temperature. The absorption spectra are composed of five bands, a_{1-5}, due to transitions from the electronic $4f^1$ ground state to the five $5d^1$ excited state levels, while the luminescence spectra are composed of two bands, b_{1-2}, due to electronic transitions from the lowest $5d^1$ excited state level to the crystal field levels of the $^2F_{5/2}$ and $^2F_{7/2}$ ground state multiplets. All transitions, fitted with Gaussian bands, are broadened by vibronic contributions.

present only in the solution spectrum. This band is assigned to the high-wavelength band of the aqueous $[Ce(H_2O)_8]^{3+}$ ion, the minor equilibrium species to the $[Ce(H_2O)_9]^{3+}$ ion.[7,9−15] Note that the 296 nm band is close to the high-wavelength band of $[Ce(H_2O)_8]^{3+}$ in **4** at 290 nm and that the four additional bands associated with the octa-aqua ion in solution overlap with the bands of the nona-aqua species at lower wavelengths.

The luminescence spectra of Ce^{3+} in **2** and **4** and in aqueous solution appear as two broad and overlapping bands, originating from the $5d^1$-$4f^1$ ($^2F_{5/2}$, $^2F_{7/2}$) transitions (Figure 2; discrete crystal-field levels are not resolved). The energy difference between these bands matches the splitting due to the spin–orbit coupling of the $^2F_{5/2}$ and $^2F_{7/2}$ levels. Both bands are subject to large Stokes shift relative to their absorption spectra, even though the shift is significantly larger for the nonahydrate. It is noteworthy that the absorption spectra of **2** and the aqueous solution are similar, while their luminescence spectra are quite different. In contrast, although the absorption spectra of **4** and the aqueous solution are very different their luminescence spectra are very similar. This is understood in terms of a fast structure change of the photoexcited $[*Ce(H_2O)_9]^{3+}$ ion as it undergoes a larger change in solution than in **2**. The magnitude of structure

DOI: 10.1021/acs.inorgchem.8b01224
Inorg. Chem. 2018, 57, 10111–10121

change appears to be directly related to the Stokes shift. Thus, the largest Stokes shift observed for the aqueous solution, ~10 100 cm^{-1}, is probably due to a photodissociation of an aqua ligand. A markedly smaller shift is observed for the more constraint geometry of $[*Ce(H_2O)_9]^{3+}$ (**2**), ~7800 cm^{-1}, while the smallest shifts is for $[*Ce(H_2O)_8]^{3+}$ (**4**), ~5500 cm^{-1}. Since the luminescence spectra of the aqueous solution and **4** are very similar, we assume their excited state structures are also similar, while the fact that the luminescence spectrum of **2** is different from those of **4** and the solution is understood as the degree of freedom of structural change being smaller in **2** than in the solution. The exploration of the absorption and luminescence spectra of the octa- and nona-hydrate Ce^{3+} ions in **2** and **4** constitute a striking argument for suggesting that the absorbed photon of the 4f-5d transition drives the expelling of an aqua ligand from the $[*Ce(H_2O)_9]^{3+}$ ion in aqueous solution and that emission takes place from the resulting $[*Ce(H_2O)_8]^{3+}$ species, in accord with previous decay and rise transient studies by Kaizu et al.[11] It is reasonable that the large Stokes shift reflects emission from a $[*Ce(H_2O)_8]^{3+}$ ion since the eight-coordinate ion has shorter mean Ce−O bond distances and hence a stronger ligand field compared to the absorbing nine-coordinate $[*Ce(H_2O)_9]^{3+}$ ion. This will be discussed in more detail in the theory section below.

Previous attempts to derive the luminescence lifetime of the excited $[*Ce(H_2O)_9]^{3+}$ ion in aqueous solution failed.[11] However, a lifetime of 430 ps was obtained for this ion in ethylene glycol. This is about 100 times shorter than the lifetime of the dissociated $[*Ce(H_2O)_8]^{3+}$ species in aqueous solution, 45 ns,[11] and virtually the same value as in the present study, 44.6 ± 0.1 ns, while the luminescence lifetimes of **2** and **4** are determined to be 35.6 ± 0.1 ns and 31.6 ± 0.1 ns, respectively (Figure S7; Table S5). It should be mentioned that the luminescence lifetime of $Ce^{3+}(aq)$ in D_2O is the same as in H_2O,[22] indicating that the transitions between the excited state ($^2D_{3/2}$) and the ground state ($^2F_{7/2}$, $^2F_{5/2}$) multiplets do not involve coupling with O−H vibrational overtones. This is understood in terms of a large energy gap (~27 500 cm^{-1}) between the $^2D_{3/2}$ and $^2F_{7/2}$, states, making such multiphonon energy transfer implausible. Indeed, the quantum yield for the hydrated Ce^{3+} ion in dilute aqueous solution is nearly 100% at room temperature.[13,23]

Thermodynamics of the Hydration Equilibrium. Absorption spectra of the aqueous cerium(III) solution were measured at different temperatures between 10 and 90 °C to derive thermodynamic quantities for the hydration equilibrium of eq 1 (Figure 3a). Minor changes are seen in the spectra with increasing temperature, indicating that the $[Ce(H_2O)_9]^{3+}$ ion is the main species also at 90 °C; however, the small increase of the 295 nm band and the simultaneous decrease of the 253 nm band with increasing temperature indicates that the fraction of $[Ce(H_2O)_8]^{3+}$ increases while that of $[Ce(H_2O)_9]^{3+}$ decreases with increasing temperature. It is not possible to acquire the wavelength-dependent molar absorptivity coefficients (ε_λ) of the individual species directly from the spectra, hindering an assessment of their molar concentration as a function of temperature. However, by assuming similar spectral envelopes for the nona- and octa-aqua ions in solution as for **2** and **4**, respectively, and by analyzing the changes in the molar absorptivity for these species as a function of temperature, the molar absorptivity ratio $\varepsilon_{255}/\varepsilon_{295}$ could be determined and thus the corresponding mole ratios $K = [Ce(H_2O)_8]^{3+}/[Ce(H_2O)_9]^{3+}$ (Figure 3b). A detailed description of this analysis

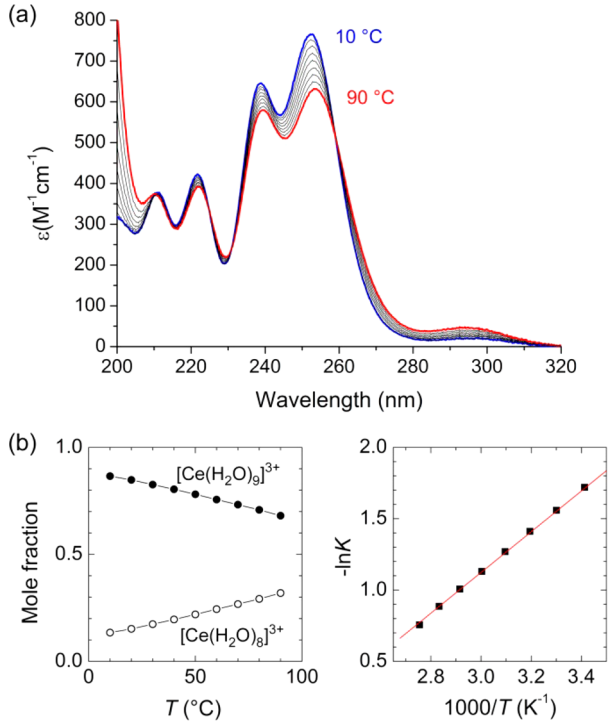

Figure 3. (a) 4f-5d absorption spectra of Ce^{3+} in dilute aqueous solution (1.80 mM $CeCl_3$ in 20 mM HCl) at 10−90 °C. (b) Relative concentration of the aqueous $[Ce(H_2O)_9]^{3+}$ and $[Ce(H_2O)_8]^{3+}$ species as a function of temperature. (c) Van't Hoff linear representation $-\ln K$ vs $1/T$. Linear regression yields $\Delta H° = 11.9 \pm 0.8$ kJ mol^{-1}; $\Delta S° = 26.3 \pm 1.6$ J mol^{-1} K^{-1} (Table 1). The estimated error in K (10−90 °C) is ±0.2.

is provided in the Supporting Information. An astonishing result is that ε_{255} is about six times larger than ε_{295}. Therefore, the molar fraction of the octaaqua species appears to be about six times smaller than its actual concentration. The molar fractions of both species derived from the spectra of the solutions enable us to calculate the equilibrium constant $K(T)$ of eq 1, assuming a water activity equal to unity. By plotting $-\ln K$ versus T^{-1} (Figure 3c) and by applying the Van't Hoff equation (eq 2) we obtain values for the enthalpy and entropy that are in good agreement with those published previously for Ce^{3+} and more recently for Cm^{3+} (Table 1);[6a,12,15] thus, for

Table 1. Thermodynamic Data Associated with eq 1 from Variable-Temperature and Variable-Pressure Studies of Ce^{3+} and Cm^{3+} Ions in Aqueous Solution

	Ce^{3+} (exp)	Cm^{3+} (exp)[d]
$\Delta H°$ (kJ mol^{-1})	+11.9 ± 0.08;[a] + 13[b]	+13.1 ± 0.4
$\Delta S°$ (J mol^{-1} K^{-1})	+26.3 ± 1.6;[a] + 33[b]	+25.4 ± 1.2
$\Delta V°$ (cm^3 mol^{-1})	+10.9 ± 0.3[c]	
$K(298)$	0.20 ± 0.03;[a] 0.28;[b] 0.21 ± 0.03[c]	0.11 ± 0.02

[a]This study. [b]Ref 12. [c]Ref 15. [d]Ref 6a.

Ce^{3+} $\Delta G°$ (298 K) = 4.1 ± 0.02 kJ mol^{-1}. This is comparable with the value derived with ab initio (MP2) methods, 2.6 kJ mol^{-1} (see the Supporting Information for details).

$$-\ln K = \Delta G°/RT = \Delta H°/RT - \Delta S°/R \quad (2)$$

DOI: 10.1021/acs.inorgchem.8b01224
Inorg. Chem. 2018, 57, 10111−10121

Inner-Sphere Cerium-Chloride Complexes. The chloride ion was earlier considered to form only outer-sphere complexes with trivalent lanthanide and actinide ions in aqueous solution, even in concentrated solutions.[24] This view, however, was soon questioned and several authors have since then reported inner-sphere Ln-Cl and An-Cl complexes.[4,25] In a recent Raman study on the hydration and ion-pair formation of the early Ln^{3+} ions in aqueous solution, $[Ce(H_2O)_{9-n}Cl_n]^{+3-n}$ (n = 1, 2) species were claimed to be the main species in an aqueous 2 M $CeCl_3$ + 4 M HCl solution.[25b] However, we will show below that eight-coordinate chloro-species are significant in these solutions. In contrast, Kanno et al.[26] did not consider chloro-species in their Raman study of aqueous $EuCl_3$ solutions at high concentration. They explained the appearance of an additional band in the Eu−O stretching region with an increase of the $[Eu(H_2O)_9]^{3+}$ mole fraction on the expense of $[Eu(H_2O)_8]^{3+}$. This effect was named "the anomalous concentration dependence" as it appeared to go against the mass-action law with respect to the decreasing water activity upon increasing chloride concentration (cf., eq 1).

Figure 4 compares the 4f-5d absorption and luminescence spectra of Ce^{3+} in a saturated yttrium chloride aqueous solution with those of the models of $[Ce(H_2O)_7Cl_2]^+$, $[Ce(H_2O)_7Cl]^{2+}$, and $[Ce(H_2O)_6Cl_2]^+$ in **3**, **5**, and **6**, respectively. It is clearly seen that a significant amount of inner-sphere Ce−Cl complexes is present in the solution. The most apparent signatures for this include a rather strong absorption and a red-shift of the high-wavelength band as well as alterations of the bands at lower wavelengths. Comparison of the absorption and luminescence spectra of the aqua-chloro species of the solids in Figure 4 and the homoleptic aqua species in Figure 2 provides insight into the coordination chemistry of the chloro-species in aqueous solution. Thus, since the eight-coordinate $[Ce(H_2O)_7Cl]^{2+}$ (**5**) and $[Ce(H_2O)_6Cl_2]^+$ (**6**) species have pronounced absorption bands at 289 and 311 nm, respectively, and the corresponding band of the solution species is at 306 nm, and because the absorption spectrum of $[Ce(H_2O)_9]^{3+}$ in dilute aqueous solution is similar to that of $[Ce(H_2O)_7Cl_2]^+$ (**3**), we conclude that the mixed aqua-chloro species are mainly eight-coordinate mono- and dichloro species, $[Ce(H_2O)_7Cl]^{2+}$ and $[Ce(H_2O)_6Cl_2]^+$. Nine-coordinate complexes $[Ce(H_2O)_8Cl]^{2+}$ and $[Ce(H_2O)_7Cl_2]^+$ may also occur, although their significance are not easily assessable because of their similar absorption spectra to $[Ce(H_2O)_9]^{3+}$ (cf., Figures 2 and 4).

The Stokes shifts of $[Ce(H_2O)_7Cl_2]^+$ (**3**) and $[Ce(H_2O)_7Cl]^{2+}$ (**5**) are 8180 and 5390 cm^{-1}, respectively. In agreement with the homoleptic aqua species, the Stokes shift is larger in nine-coordination than in eight-coordination (cf., Figures 2 and 4 and Table S6). The luminescence spectra of $[Ce(H_2O)_7Cl_2]^+$ (**3**) and $[Ce(H_2O)_9]^{3+}$ (**2**) are similar, both appearing at lower wavelengths than those of $[Ce(H_2O)_7Cl]^{2+}$ and $[Ce(H_2O)_8]^{3+}$ (cf., Figures 2 and 4). This is in accord with the corresponding absorption spectra, where the binding to one or two chloride ions does not change the spectrum significantly from those of the nona- and octa-aqua ions. It is rather the change in coordination number that gives rise to a significant spectral change.

Outer-Sphere Cerium-Perchlorate Complexes. A different situation takes place at high perchlorate ion concentration. We studied the effect perchlorate ions on the absorption spectra of $[Ce(H_2O)_9]^{3+}$ in aqueous solutions at different concentrations of $NaClO_4$ and $HClO_4$. In both electrolytes perchlorate is a weakly coordinating ion. Inner-sphere cerium-perchlorate complexes are only seen in the concentrated electrolytes, while various degrees of outer-sphere complexes are present in solution over a wide range of perchlorate ion concentrations, ~1−7 M (Figure 5 and Figures S8−S9). Obviously, these outer-sphere complexes do not change significantly the coordination geometry of the $[Ce(H_2O)_9]^{3+}$ ion in solution. In fact, the weak hydrogen bonding between the nona-aqua cerium(III) ion and perchlorate ions in the second coordination shell, $[Ce(H_2O)_9]^{3+}\cdots(ClO_4^-)_x$, stabilizes the nona-aqua species, which results in a shift of the equilibrium of eq 1 to the left. This is clearly seen in the absorption spectra by a decrease of the 296 nm band with increasing perchlorate ion concentration. The effect is apparent already at 1 M $NaClO_4$, and at ~7 M the band it has nearly vanished (Figure 5). Similarly, by increasing the concentration of $La(ClO_4)_3$ to a Ce^{3+} solution increases the mole fraction of $[Ce(H_2O)_9]^{3+}$ and $[La(H_2O)_9]^{3+}$ species by forming weak

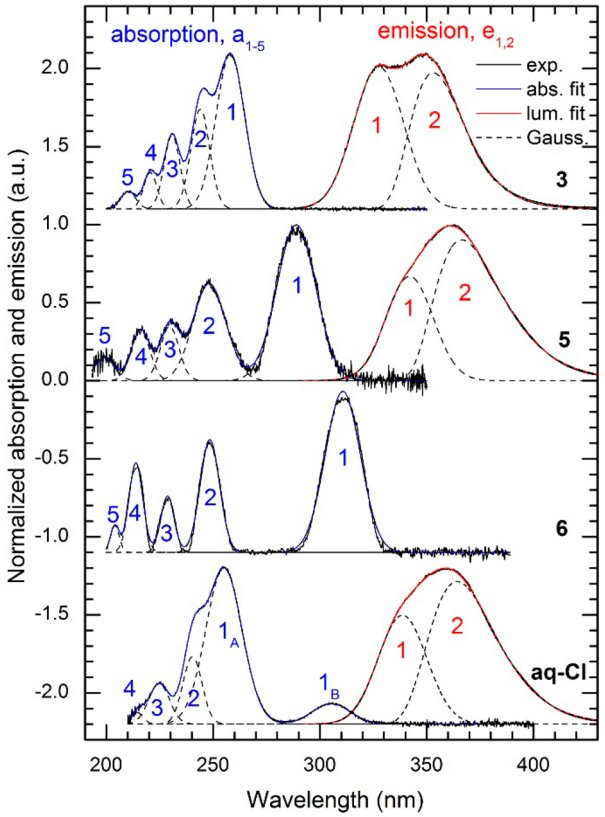

Figure 4. Comparison of the 4f-5d absorption and luminescence spectra of $[Ce(H_2O)_7Cl_2]^+$ (**3**), $[Ce(H_2O)_7Cl]^{2+}$ (**5**), $[Ce(H_2O)_6Cl_2]^+$ (**6**), and Ce^{3+} in aqueous yttrium chloride solution (**aq-Cl**, 1.3 mM $CeCl_3$ in ~1.5 M YCl_3) at room temperature. The absorption spectra are composed of five bands, a_{1-5}, due to transitions from the electronic $4f^1$ ground state to the five $5d^1$ excited state levels, while the luminescence spectra are composed of two bands, b_{1-2}, due to transitions from the lowest $5d^1$ excited level to the $^2F_{5/2}$ and $^2F_{7/2}$ multiplets of the ground state. All transitions are broadened by vibronic contributions and fitted with Gaussian bands. The absorption band labeled 1_B is due to transitions from the ground state to the lowest excited state energy level of eight-coordinate mono- and dichloro species in the solution, $[Ce(H_2O)_7Cl]^{2+}$ and $[Ce(H_2O)_7Cl_2]^+$; 1_A denotes the corresponding transitions of $[Ce(H_2O)_9]^{3+}$ species, possibly overlapping with nine-coordinate mixed mono- and dichloro $[Ce(H_2O)_8Cl]^{2+}$ and $[Ce(H_2O)_6Cl_2]^+$ species.

DOI: 10.1021/acs.inorgchem.8b01224
Inorg. Chem. 2018, 57, 10111−10121

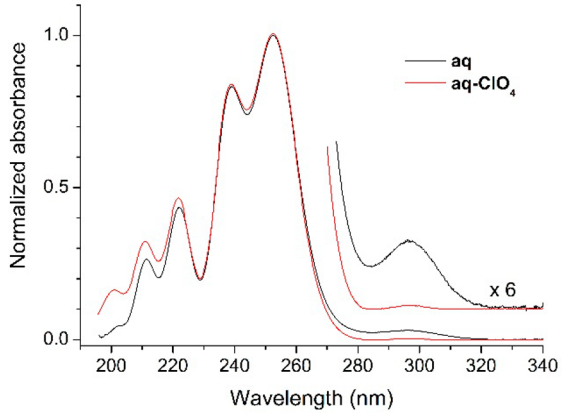

Figure 5. 4f-5d absorption spectra of 1.3 mM Ce^{3+} in 10 mM $HClO_4$ (**aq**) and in dilute 7 M $NaClO_4$ (**aq-ClO$_4$**).

hydrogen bonds to the ClO_4^- ions in the second shell. In these cases the concept of "the anomalous concentration dependence" is suitable. Note that inner-sphere complexes with perchlorate ions are present only in concentrated perchloric acid where the water activity is critically low.

Quantum Chemical Calculations. Despite the converging experimental results on the absorption and luminescence properties of the hydrated Ce^{3+} in aqueous solution and in the crystal hosts, all pointing to the fact that the coordination geometry has a direct bearing on the absorbing energy levels, and that photoabsorption of the $[Ce(H_2O)_9]^{3+}$ ion in aqueous solution induces a dissociation process of an aqua ligand and thereby a large Stokes shift, some important questions remain unanswered: For example, (i) what is the nature of the dissociation states? That is, which of the $4f^1$-$5d^1$ transitions are "chemically active"? (ii) What are the structures or the transient cerium(III) aqua complexes in the excited $5d^1$ state? (iii) What is the influence of H_2O and Cl^- ligands on the absorption and luminescence spectra of the Ce^{3+} ion in aqueous solution?

Ground State Geometries and Absorption Spectra. Realistic geometries of the first coordination shells of cerium in **1**−**6** are extracted from the crystallographic data of the hosts and scaled to match the difference in the ionic radii between Ce^{3+} and the host metal ion. The scaled structures are labeled **1a**−**6a**. In order to study the effect of the Ce−O and Ce−Cl bond distances on the absorption spectra for the six coordination figures, clusters with longer and shorter bond distances around the ideal distances are also investigated (Tables S7−S12). To assess the accuracy of this methodology before exploring the excited state properties in the next section, a direct comparison between the experimental and computed absorption spectra is necessary.

Theoretical absorption spectra of Ce^{3+} in **1a**−**6a** were computed with quantum chemical modeling tools using wave function approaches, including static and dynamic correlation effects as well as relativistic effects. Details for the calculations using spin−orbit multistate complete active space with second order perturbation theory (SO-CASPT2) methods, treating the water solvent as a polarizable continuum dielectric medium (PCM), are provided in the Supporting Information. The computed absorption spectra of **1a**−**6a** are compared together with the measured spectra of **1**−**6** in Figure 6. Although the relative intensities for some bands are not well reproduced the peak positions of the calculated and the measured absorption spectra are generally in good agreement, indicating that the coordination geometry of the cerium clusters mimic well those of the hosts. In particular, the simulations show that the high wavelength band of the nine-coordinate clusters scaled on the real structures in the crystal hosts is positioned between 250 and 260 nm, whereas for the scaled eight-coordinate clusters this band is found between 295 and 320 nm (Tables S7−S12). It is striking that when replacing successively one and two water molecules by chloride ions our calculations are able to

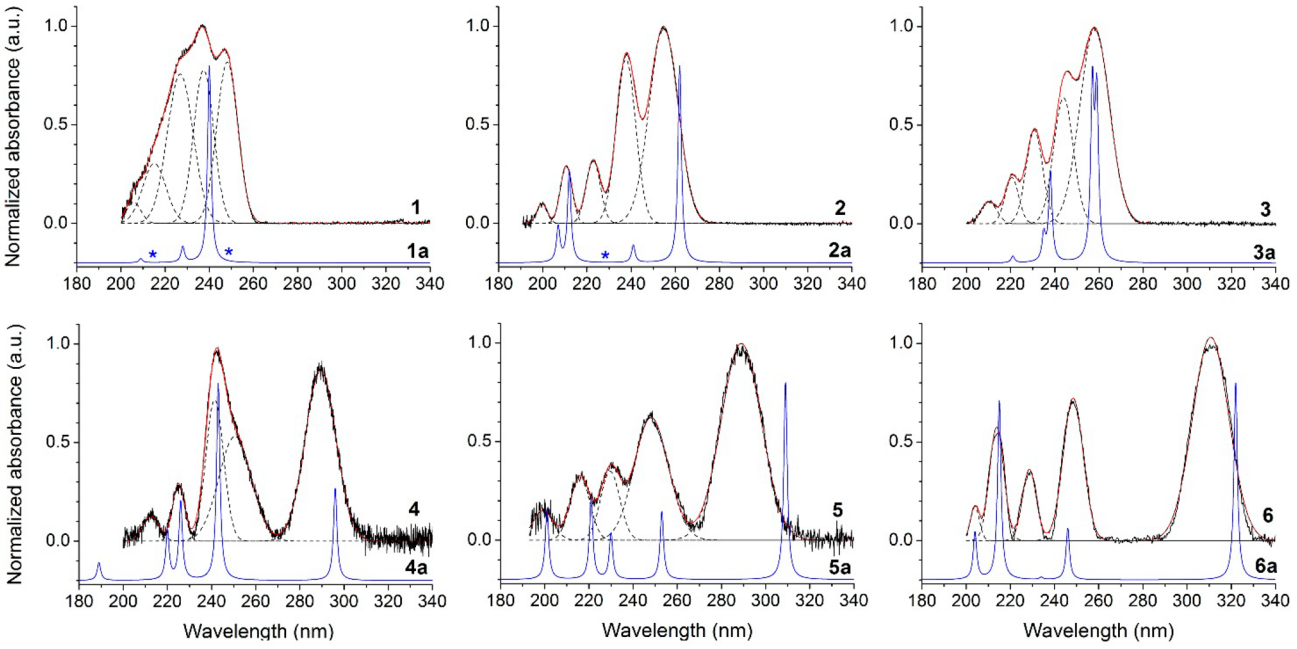

Figure 6. $4f^1$-$5d^1$ electronic absorption spectra of Ce^{3+} in **1**−**6** at room temperature. The spectra are curve-fitted with Gaussian component band to represent the transitions to the five $5d^1$ states. The corresponding theoretical spectra (calculated at the SO-CASPT2 level; see text) are shown in blue lines. The symbol * refers to dark states with very low or zero oscillator strengths.

DOI: 10.1021/acs.inorgchem.8b01224
Inorg. Chem. 2018, 57, 10111−10121

reproduce the enhancement of the intensity and the red-shift of the high wavelength band observed experimentally by increasing chloride concentration (cf., Figures 2, 4, and 6 and the transition values of **4a**, **5a**, and **6c** in Tables S9−S11).

It is interesting to note that the calculated oscillator strength of the transition to the lowest $5d^1$ level of $[Ce(H_2O)_9]^{3+}$ (**2a**) is about three times larger than for $[Ce(H_2O)_8]^{3+}$ (**4a**) (cf., Tables S8 and S10). This may be compared with the molar absorptivities of the corresponding transitions for the nona- and octahydrate ions in solution, where ε_{255} for the former is almost six times larger than ε_{296} for the latter. The calculations also provide insight into the presence of electronic states associated with low or zero oscillator strengths, so-called dark states. These are very sensitive to even small changes in the coordination geometry.

Chemical Bond Analysis of Ground State and Excited State Structures. The fact that the fully hydrated and the mixed aqua-chloro complexes have similar UV absorption spectra in nine- and eight-coordination, respectively, indicates that these complexes have similar ligand-field strengths (Figure 6), although a small red-shift is seen for the high wavelength band of $[Ce(H_2O)_6Cl_2]^{+}$ (**6**/**6a**) compared to the high wavelength bands of $[Ce(H_2O)_8]^{3+}$ (**4**/**4a**) and $[Ce(H_2O)_7Cl]^{2+}$ (**5**/**5a**). To support these results we performed topological analysis of electron charge densities along the Ce−O and Ce−Cl bonds in optimized structures of $[Ce(H_2O)_9]^{3+}$, $[Ce(H_2O)_7Cl_2]^{+}$, $[Ce(H_2O)_8]^{3+}$, and $[Ce(H_2O)_7Cl]^{2+}$ using quantum theory of atoms in molecules (QTAIM) analysis; the results are summarized in Table S13. This enabled us to probe the nature of the bonds and to which extent they are influenced by the coordination geometry and the ligand stoichiometry. At the bond critical point (BCP) the density ρ_b, its Laplacian $\nabla^2\rho_b$, and the energy density H_b are in the range usually observed for electrostatic type of bonds.[27] In the ground state of $[Ce(H_2O)_9]^{3+}$ with tricapped trigonal prismatic geometry, the Ce−O bonds to the capping water molecules are slightly longer and thus a little more ionic than the bonds to the prismatic water molecules. This is reflected in the slightly smaller ρ_b value for the capping bonds (0.037 e^-/bohr^3) relative to the prismatic bonds (0.039 e^-/bohr^3), in agreement with the recent results of Zhang et al.[28] In comparison, the shorter Ce−O bonds in $[Ce(H_2O)_8]^{3+}$ correspond to a slightly larger ρ_b value (0.041 e^-/bohr^3) than that of the capping bonds in $[Ce(H_2O)_9]^{3+}$. Interestingly, ρ_b is slightly larger for the Ce−O (0.046 e^-/bohr^3) and Ce−Cl (0.049 e^-/bohr^3) bonds in $[Ce(H_2O)_7Cl]^{2+}$, indicating marginally less ionic bond character than in $[Ce(H_2O)_8]^{3+}$; indeed, the two species have very similar absorption spectra (Figure 6).

Natural bond orbital (NBO) population and charge analysis confirm the results from the QTAIM calculations (Tables S13−S14). Notably, the analysis indicate significant electron backdonation from the ligands to the cerium 5d orbitals in the ground states of $[Ce(H_2O)_8]^{3+}$, $[Ce(H_2O)_9]^{3+}$, and $[Ce(H_2O)_7Cl_2]^{+}$, which is particularly pronounced for the aqua-chloro complex. This is also reflected in a lower natural charge of cerium in this complex compared to the nona- and octa-aqua hydrates. Upon excitation the occupation of the 4f orbitals decreases by nearly one electron unit in all three complexes, while the 5d orbital population increases by the roughly the same amount. The excitation also decreases the natural charge on cerium by about 0.2 and 0.4 electron unit for the octa- and nonahydrates, respectively, while the value for the aqua-chloro complex is about 0.3 electron units (Table S14). In comparison, these charge changes are larger than those reported for various cerium(III) guanidinate-amide complexes (0.1−0.2).[8d]

Excited State Reactivity and Electronic Absorption and Emission Spectra. To explore theoretically the dissociative reaction where an aqua ligand molecule is expelled from the $[*Ce(H_2O)_9]^{3+}$ ion in the excited $5d^1$ state we used time-dependent density functional theory (TD-DFT) with the PBE0 functional to compute the potential energy surface of the $5d^1$ excited states and to optimize the transient geometries of the dissociation reaction without constraints (see the Supporting Information for details). TD-DFT was also used to explore the excited state reactivity of $[*Ce(H_2O)_8]^{3+}$ and $[*Ce(H_2O)_7Cl_2]^{+}$. The PBE0 functional was found to be accurate enough to reproduce the spin-free MS-CASPT2 $4f^1$-$5d^0 \rightarrow 4f^0$-$5d^1$ electronic absorption spectrum and preventing ligand-to-metal charge-transfer transitions to spuriously occur in the $5d^1$ state manifolds of $[*Ce(H_2O)_9]^{3+}$, $[*Ce(H_2O)_8]^{3+}$, and $[*Ce(H_2O)_7Cl_2]^{+}$ (neither did this occur in the wave function calculations; see Table S15).

$[*Ce(H_2O)_9]^{3+}$. In all the $5d^1$ excited states of this ion with regular tricapped trigonal prismatic geometry (D_{3h}) the unpaired electron occupies the $5d^1$ orbitals with antibonding character with respect to the oxygen atoms of the water molecules (Figure 7). Table S18 shows that the first spin-free

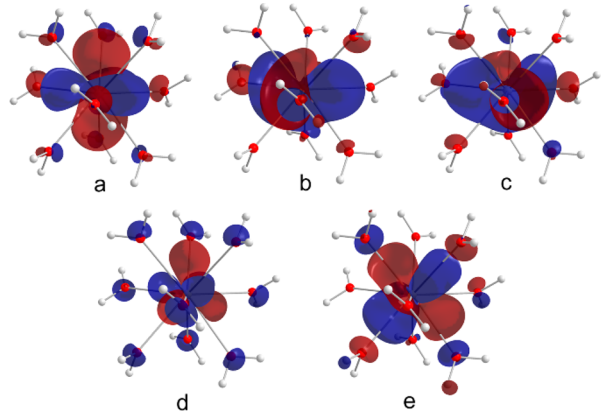

Figure 7. Plots of the natural transition orbitals computed at the TD-DFT PBE0 level of theory for the five $5d^1$ excited states of $[*Ce(H_2O)_9]^{3+}$ in D_{3h} point group. The isosurface cutoff is 0.03 au.

5d state of the $[Ce(H_2O)_9]^{3+}$ complex, corresponding to the excitation in the orbital (a) depicted in Figure 7, is well-separated from the other excited 5d states by about 1000 cm^{-1}. When the geometry of the model system is relaxed in this lowest energy level of the $5d^1$ state, the capping water molecule leaves the $[*Ce(H_2O)_9]^{3+}$ complex along a barrier-less energy profile, leading to a local minimum of a $[*Ce(H_2O)_8]^{3+}\cdot H_2O$ complex, stabilized by hydrogen bonds between the distant water molecule and two water molecules of the first coordination shell of the octahydrate ion. The ligand dissociation gives rise to a compression of the coordination shell; the mean Ce−O bond distances for the nine- and eight-coordinate species are 2.57 and 2.53 Å, respectively (see Figure 8a−c and the movie in the Supporting Information). Note that there is no crossing of the energy levels in the transient structures. In addition, absorption into the higher four $5d^1$ states does not result in photodissociation (Figure 8c). This

DOI: 10.1021/acs.inorgchem.8b01224
Inorg. Chem. 2018, 57, 10111−10121

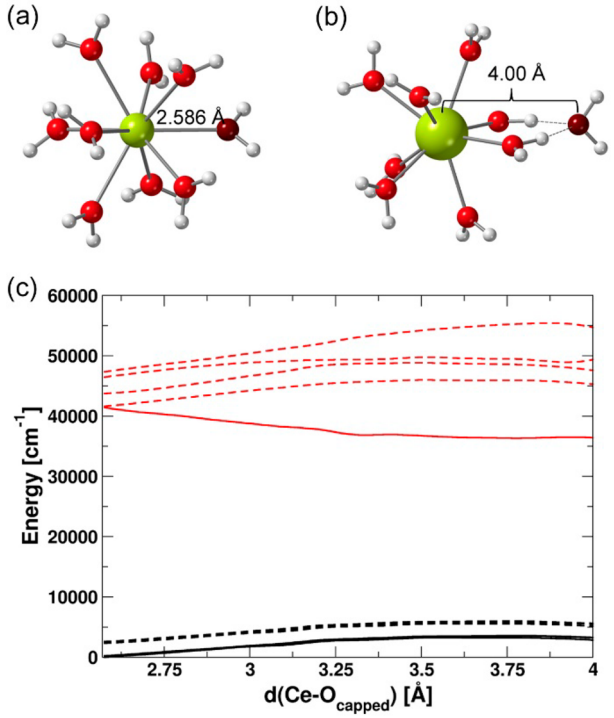

Figure 8. Perspective views of (a) the early excited state complex $[*Ce(H_2O)_9]^{3+}$ with regular tricapped trigonal prismatic geometry and (b) the "product" $[*Ce(H_2O)_8]^{3+}\cdot H_2O$ complex with distorted geometry as a result of a capped water molecule (its oxygen atom is depicted in dark red color) is pulled out from $[*Ce(H_2O)_9]^{3+}$. (c) Potential energy curves computed at the SO-CASPT2 level along the dissociative Ce−O (capped) pathway; $4f^1$ states are drawn with black lines, the four highest $5d^1$ states with red dashed lines, while the lowest $5d^1$ state which has a dissociative character is drawn with a plain thick red line. Note the interchange between the lowest and the second lowest states through the reaction path.

model can explain the principal transient dynamics of the $5d^1$ excited state of the $[*Ce(H_2O)_9]^{3+}$ ion in aqueous solution and in **1** and **2**. In solution the expelled water molecule enters the second coordination shell where it is stabilized by hydrogen bonds to neighbor water molecules, while in the two solids the expelled water molecule cannot entirely enter the second shell due to crystal constraints. However, modeling the transient structures of these large molecular systems is beyond the scope of this paper.

Emission spectra corresponding to transitions from the lowest $5d^1$ energy state to the seven $4f^0$ states were computed for both the reactant $[*Ce(H_2O)_9]^{3+}$ ($5d_0$ orbital) and the product $[*Ce(H_2O)_8]^{3+}\cdot H_2O$ (mixture of $5d_0$ and $5d_{-2}$ orbitals) at the SO-CASPT2 level. The reactant, still in its ground-state geometry, is short-lived.[11] Its emission bands are grouped between 250 and 270 nm, even though some of them have small or zero oscillator strengths. The zero-phonon lines of the emission and absorption spectra of $[Ce(H_2O)_9]^{3+}$ and $[*Ce(H_2O)_9]^{3+}$, respectively, overlap at 249 nm; hence, there is no Stokes shift. In contrast, the emission zero-phonon line of $[*Ce(H_2O)_8]^{3+}\cdot H_2O$ appears at significantly longer wavelength (299 nm) compared to the absorption zero-phonon line, giving a Stokes shift of about 6800 cm^{-1}. The experimental value of the Stokes shift for Ce^{3+} in aqueous solution is ∼10 100 cm^{-1}; cf. Figure 2, Figure S13, Table S6, and Table S15. The computed emission lines are distributed in two groups at about 300 and 322 nm, corresponding to the $^2F_{5/2}$ and $^2F_{7/2}$ states (Figure S13; Table S15). The splitting between these, due to spin−orbit coupling, amounts to ∼2275 cm^{-1}. This is similar to the experimental value of the $[*Ce(H_2O)_8]^{3+}$ ion in aqueous solution, ∼2100 cm^{-1}, even though the luminescence peak maximum for the aqueous solution is red-shifted relative to the computed emission spectrum.

$[*Ce(H_2O)_8]^{3+}$. While excitation into the lowest $5d^1$ state of the nona-aqua cerium(III) ion with tricapped trigonal prismatic geometry results in an instant dissociation of an aqua ligand, excitation into the same $5d^1$ state of $[Ce(H_2O)_8]^{3+}$ with square antiprismatic structure results in a contraction of the Ce−O bond distances by 0.083 Å (average value). This large contraction the increases ligand field strength around cerium significantly, which is the main reason for the large red-shift of the emission spectrum relative to its absorption spectrum with a computed Stokes shift in the range 3372−6452 cm^{-1}. This may be compared with measured Stokes shift in **4**, ∼5450 cm^{-1}.

$[*Ce(H_2O)_7Cl_2]^{+}$. Similar to the nonahydrate ion, TD-DFT optimization of the first $5d^1$ excited state of the $[*Ce(H_2O)_7Cl_2]^{+}$ species results in a fast, barrier-less dissociation of an aqua ligand. A stable product (local minimum) is reached with the dissociated water molecule hydrogen-bonded to a water molecule of the first coordination shell of a $[*Ce(H_2O)_6Cl_2]\cdot H_2O$ species (Figure 9). Its emission spectrum is shown together with the absorption spectrum of $[Ce(H_2O)_7Cl_2]^{+}$ in Figure S13. The Stokes shift in this system amounts to about 12 300 cm^{-1}, which is even larger than that for the nona-aqua ion discussed above (cf., Table S15 and Table S16).

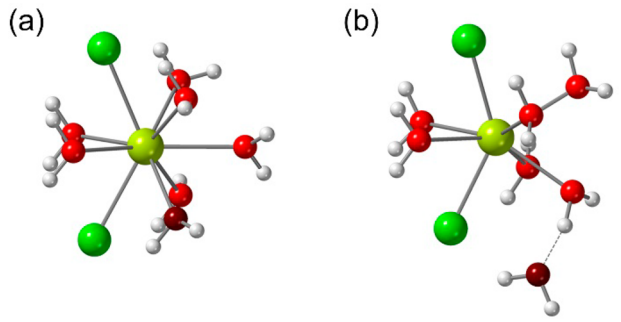

Figure 9. Perspective views of (a) the early excited state complex $[*Ce(H_2O)_7Cl_2]^{+}$ and the "product" $[*Ce(H_2O)_6Cl_2]^{+}\cdot H_2O$ (the oxygen atom of the dissociated water molecule is marked in dark red color).

These quantum chemical results strongly support that the luminescence of the $[*Ce(H_2O)_9]^{3+}$ ion in solution is driven by a photochemical dissociation a water molecule to produce a more stable $[*Ce(H_2O)_8]^{3+}$ complex at which the luminescent occurs. The large Stokes shift in this system is therefore a consequence of two effects: first a change in the coordination number from nine to eight causing a decrease in the mean Ce−O distance and an increase of the ligand field strength, then a further contraction of the eight-coordinate structure and thus a further increase of the ligand field strength. In a recent paper by Qiao el al. on various Ce(III) guanidinate-amide complexes with coordination numbers from three to six, the Stokes shifts were found to be smaller for the complexes with higher coordination numbers.[8d] However, when considering that

DOI: 10.1021/acs.inorgchem.8b01224
Inorg. Chem. 2018, 57, 10111−10121

those complexes undertook a smaller contraction of the Ce−N bonds than did the complexes with lower coordination numbers, the results are comparable with the present results.

CONCLUSION

We have recorded and analyzed the Ce^{3+} 4f-5d absorption and luminescence spectra of $[Ce(H_2O)_9]^{3+}$ and $[Ce(H_2O)_8]^{3+}$ complexes as well as eight- and nine-coordinate mixed aqua-chloro complexes in well-characterized crystal structures. The measured absorption spectra were compared with theoretical spectra from accurate quantum chemical electronic structure calculations of cerium(III) clusters mimicking those in the real crystal structures. The computed and the measured absorption spectra are in excellent agreement, both of which clearly showing that the coordination polyhedron and the point symmetry considerably influence the positions and the intensities of the absorption bands. Thus, the position of the low energy 5d absorption band of the eight-coordinate homoleptic aqua complex and the mixed aqua-mono/dichloro complexes are lower in energy compared to the nine-coordinate complexes. This is clearly seen as a pronounced band at 289 nm in the absorption spectra of $[Ce(H_2O)_8]^{3+}$ and $[Ce(H_2O)_7Cl]^{2+}$, near 310 nm for $[Ce(H_2O)_6Cl_2]^{+}$, while the corresponding bands for the nine-coordinate complexes $[Ce(H_2O)_9]^{3+}$ and $[Ce(H_2O)_7Cl_2]^{+}$ are between 248 and 258 nm. This means that it is possible to distinguish between nine- and eight-coordinate Ce^{3+} aqua species in solution, whereas the spectroscopic differences between homoleptic aqua complexes and mixed aqua-chloro complexes are less pronounced.

The information derived from the absorption spectra of the nona- and octahydrate model structures were used for deconvolution of the absorption spectrum of the Ce^{3+} aqueous solution into $[Ce(H_2O)_9]^{3+}$ and $[Ce(H_2O)_8]^{3+}$ complexes at different temperatures between 10 and 90 °C. This information was further used to obtain enthalpy and entropy values for the equilibrium between nona- and octahydrate species in solution. The molar fraction of the latter is ∼0.13 at 10 °C but increases to ∼0.32 at 90 °C, indicating an entropy driven reaction.

The absorption spectra (but not the luminescence spectra) of Ce^{3+} in aqueous solutions at high chloride concentration clearly show evidence of eight-coordinate Ce−Cl inner-sphere species (contact ion-pairs), whereas the contribution of nine-coordinate Ce−Cl complexes is not easily distinguished from the nona-aqua species. In contrast, in solutions at high perchlorate ion concentration Ce^{3+}-H_2O-ClO_4^- outer-sphere complexes (solvent-shared ion pairs) are formed. The absorption spectra of these are very similar and cannot be distinguished from the absorption spectra of the aqueous $[Ce(H_2O)_9]^{3+}$ species. The fact that these solvent-shared ion pairs stabilize the nona-aqua ion and destabilize the octa-aqua ion (the 295 nm band, assigned to the octa-aqua ion, decreases upon increasing perchlorate concentration) is evidence for their presence in these systems.

QTAIM analysis demonstrates that for the Ce^{3+} octa and nonahydrate complexes and the mixed aqua-chloro complexes the Ce−O and Ce−Cl bonds are ionic and have comparable bond strengths. This is consistent with that the absorption spectra of the nine-coordinate $[Ce(H_2O)_9]^{3+}$ and $[Ce(H_2O)_7Cl_2]^{+}$ species in **2** and **3**, respectively, are very similar. Likewise, the spectra of $[Ce(H_2O)_8]^{3+}$ and $[Ce(H_2O)_7Cl]^{2+}$ in **2** and **3**, respectively, are similar to each other but very different from those of the nine-coordinate species.

These quantum chemical calculations also reveal that among the five $5d^1$ excited state levels of the $[*Ce(H_2O)_9]^{3+}$ ion the lowest level has the largest oscillator strength and intrinsic dipole moment. Upon excitation, this ion relaxes vibrationally via a barrier-less process that results in a photodissociated eight-coordinate $[*Ce(H_2O)_8]^{3+}{\cdot}H_2O$ complex with a mean Ce−O bond distance that is shorter than in the initial nine-coordinate complex. The relatively large relaxation energy in this process translates to an equally large Stokes shift, ∼7000 cm^{-1}, which may be compared to the experimental value for the aqueous solution, ∼10 100 cm^{-1}. This confirms that the luminescence spectrum mainly stems from a photodissociated $[*Ce(H_2O)_8]^{3+}$ species. A similar dissociation process takes place for $[Ce(H_2O)_7Cl_2]^{+}$, where photoexcitation gives rise to a rapid ejection of an aqua ligand to produce a $[*Ce(H_2O)_6Cl_2]^{+}{\cdot}H_2O$ species. The Stokes shift in this process is ∼12 000 cm^{-1}. Thus, the large Stokes shifts observed experimentally for nine-coordinate aqua and mixed aqua-chloro Ce^{3+} complexes in aqueous solution are confirmed by theory, while for various eight-coordinate aqua complexes our quantum chemical calculations predict Stokes shifts in the range 4000−5000 cm^{-1}, showing that in eight-coordination the Stokes shift is due to a decrease of the Ce−O bonds in the excited state. For hydrated aqua and mixed aqua-chloro Ce^{3+} complexes in aqueous solution and in **2** and **3**, this study shows that there is a positive correlation between coordination numbers eight and nine and the corresponding Stokes shift. This is explained by a larger structure change of the excited state structures in nine-coordination than in eight-coordination. In aqueous solution the structure change is extreme as an aqua ligand is expelled from the first coordination shell of the $[Ce(H_2O)_9]^{3+}$ ion. That the Stokes shifts are larger for the nine-coordinate than for eight-coordinate Ce^{3+} species in the crystal structures in this study is likely due to larger structure changes in the former, although a complete ejection of aqua ligands is prohibited by crystal constrains.

ASSOCIATED CONTENT

Supporting Information

The Supporting Information is available free of charge on the ACS Publications website at DOI: 10.1021/acs.inorgchem.8b01224.

Complete set of quantum chemical Cartesian coordinates(ZIP)

Ce−O bond distances for the nine- and eight-coordinate species (ZIP)

Synthetic details and characterizations, crystal data, electronic absorption, excitation, and luminescence data, and computational details (PDF)

Accession Codes

CCDC 1823623 contains the supplementary crystallographic data for this paper. These data can be obtained free of charge via www.ccdc.cam.ac.uk/data_request/cif, or by emailing data_request@ccdc.cam.ac.uk, or by contacting The Cambridge Crystallographic Data Centre, 12 Union Road, Cambridge CB2 1EZ, UK; fax: +44 1223 336033.

AUTHOR INFORMATION

Corresponding Authors

*E-mail: patric.lindqvist@kit.edu.

DOI: 10.1021/acs.inorgchem.8b01224
Inorg. Chem. 2018, 57, 10111−10121

*E-mail: florent.real@univ-lille.fr.
*E-mail: valerie.vallet@univ-lille.fr.

ORCID

Patric Lindqvist-Reis: 0000-0001-8671-4570
Florent Réal: 0000-0002-5163-1545
Valérie Vallet: 0000-0002-2202-3858

Present Address

[#]Department of Plant Protection Biology, Swedish University of Agricultural Sciences, P.O. Box 102, 23053 Alnarp, Sweden.

Author Contributions

The manuscript was written through contributions of all authors. All authors have given approval to the final version of the manuscript.

Notes

The authors declare no competing financial interest.

■ ACKNOWLEDGMENTS

This work was partially supported by the European FP7 Talisman project under a contract with the European Commission, by LABEX CaPPA (ANR-11-LABX-0007), and by the Ministry of Higher Education and Research, Hauts de France council and European Regional Development Fund (ERDF) through the Contrat de Projets Etat-Region (CPER CLIMIBIO).

■ REFERENCES

(1) Panak, P. J.; Geist, A. Complexation and Extraction of Trivalent Actinides and Lanthanides by Triazinylpyridine N-Donor Ligands. *Chem. Rev.* **2013**, *113*, 1199−1236.

(2) (a) Knope, K. E.; Soderholm, L. Solution and Solid-State Structural Chemistry of Actinide Hydrates and Their Hydrolysis and Condensation Products. *Chem. Rev.* **2013**, *113*, 944−994. (b) Lindqvist-Reis, P.; Apostolidis, C.; Rebizant, J.; Morgenstern, A.; Klenze, R.; Walter, O.; Fanghänel, T.; Haire, R. G. The Structures and Optical Spectra of Hydrated Transplutonium Ions in the Solid State and in Solution. Angew. *Angew. Chem., Int. Ed.* **2007**, *46*, 919−922.

(3) (a) Altmaier, M.; Gaona, X.; Fanghänel, T. Recent Advances in Aqueous Actinide Chemistry and Thermodynamics. *Chem. Rev.* **2013**, *113*, 901−943. (b) D'Angelo, P.; Zitolo, A.; Migliorati, V.; Chillemi, G.; Duvail, M.; Vitorge, P.; Abadie, S.; Spezia, R. Revised Ionic Radii of Lanthanoid(III) Ions in Aqueous Solution. *Inorg. Chem.* **2011**, *50*, 4572−4579. (c) Persson, I.; D'Angelo, P.; De Panfilis, S.; Sandström, M.; Eriksson, L. Hydration of Lanthanoid(III) Ions in Aqueous Solution and Crystalline Hydrates Studied by EXAFS Spectroscopy and Crystallography: The Myth of the "Gadolinium Break. *Chem. - Eur. J.* **2008**, *14*, 3056−3066.

(4) Allen, P. G.; Bucher, J. J.; Shuh, D. K.; Edelstein, N. M.; Craig, I. Coordination Chemistry of Trivalent Lanthanide and Actinide Ions in Dilute and Concentrated Chloride Solutions. *Inorg. Chem.* **2000**, *39*, 595−601.

(5) (a) Näslund, J.; Lindqvist-Reis, P.; Persson, I.; Sandström, M. Steric Effects Control the Structure of the Solvated Lanthanum(III) Ion in Aqueous, Dimethyl Sulfoxide, and N,N′-Dimethylpropyleneurea Solution. An EXAFS and Large-Angle X-ray Scattering Study. *Inorg. Chem.* **2000**, *39*, 4006−4011. (b) D'Angelo, P.; Zitolo, A.; Migliorati, V.; Persson, I. Analysis of the Detailed Configuration of Hydrated Lanthanoid(III) Ions in Aqueous Solution and Crystalline Salts by Using K- and L_3-Edge XANES Spectroscopy. *Chem. - Eur. J.* **2010**, *16*, 684−692.

(6) (a) Lindqvist-Reis, P.; Klenze, R.; Schubert, G.; Fanghänel, T. Hydration of Cm^{3+} in Aqueous Solution from 20 to 200°C. A Time-Resolved Laser Fluorescence Spectroscopy Study. *J. Phys. Chem. B* **2005**, *109*, 3077−3083. (b) Lindqvist-Reis, P.; Walther, C.; Klenze, R.; Eichhöfer, A.; Fanghänel, T. Large Ground-State and Excited-State Crystal Field Splitting of 8-Fold-Coordinate Cm^{3+} in $[Y(H_2O)_8]Cl_3$·15-crown-5. *J. Phys. Chem. B* **2006**, *110*, 5279−5285. (c) Lindqvist-Reis, P.; Walther, C.; Klenze, R.; Edelstein, N. M. Optical Spectra and Crystal-Field Levels of $[Cm(H_2O)_9]^{3+}$ Ions with C_{3h} Symmetry in Isotypic Rare-Earth Triflate and Ethyl Sulfate Salts. *J. Phys. Chem. C* **2009**, *113*, 449−458. (d) Mondry, A.; Starynowicz, P. Ten-Coordinate Neodymium(III) Complexes with Triethylenetetraaminehexaacetic Acid. *Eur. J. Inorg. Chem.* **2006**, *2006*, 1859−1867. (e) Janicki, R.; Mondry, A. A New Approach to Determination of Hydration Equilibria Constants for the Case of $[Er(EDTA)(H_2O)_n]^-$ Complexes. *Phys. Chem. Chem. Phys.* **2014**, *16*, 26823−26831. (f) Janicki, R.; Mondry, A. Thermodynamics of the Hydration Equilibrium Derived from the Luminescence Spectra of the Solid State for the Case of the Eu-EDTA System. *Phys. Chem. Chem. Phys.* **2015**, *17*, 29558−29565.

(7) Jørgensen, C. K.; Brinen, J. S. Far Ultra-Violet Absorption Spectra of Cerium(III) and Europium(III) Aqua Ions. *Mol. Phys.* **1963**, *6*, 629−631.

(8) (a) Yin, H.; Carroll, P. J.; Manor, B. C.; Anna, J. M.; Schelter, E. J. Cerium Photosensitizers: Structure-Function Relationships and Applications in Photocatalytic Aryl Coupling Reactions. *J. Am. Chem. Soc.* **2016**, *138* (18), 5984−5993. (b) Yin, H.; Carroll, P. J.; Anna, J. M.; Schelter, E. J. Luminescent Ce(III) Complexes as Stoichiometric and Catalytic Photoreductants for Halogen Atom Abstraction Reactions. *J. Am. Chem. Soc.* **2015**, *137*, 9234−9237. (c) Yin, H.; Jin, Y.; Hertzog, J. E.; Mullane, K. C.; Carroll, P. J.; Manor, B. C.; Anna, J. M.; Schelter, E. J. The Hexachlorocerate(III) Anion: A Potent, Benchtop Stable, and Readily Available Ultraviolet A Photosensitizer for Aryl Chlorides. *J. Am. Chem. Soc.* **2016**, *138*, 16266−16273. (d) Qiao, Y.; Sergentu, D.-C.; Yin, H.; Zabula, A. V.; Cheisson, T.; McSkimming, A.; Manor, B. C.; Carroll, P. J.; Anna, J. M.; Autschbach, J.; Schelter, E. J. Understanding and Controlling the Emission Brightness and Color of Molecular Cerium Luminophores. *J. Am. Chem. Soc.* **2018**, *140*, 4588−4595. (e) Qin, X.; Liu, X.; Huang, W.; Bettinelli, M.; Liu, X. Luminescence-Activated Phosphors Based on 4f-5d Optical Transitions: Theoretical and Experimental Aspects. *Chem. Rev.* **2017**, *117*, 4488−4527.

(9) Okada, K.; Kaizu, Y.; Kobayashi, H. Aqualigand Dissociation of 5d←4f Excited $[Ce(OH_2)_9]^{3+}$ in Aqueous Solution. *J. Chem. Phys.* **1981**, *75*, 1577−1578.

(10) Okada, K.; Kaizu, Y.; Kobayashi, H.; Tanaka, K.; Marumo, F. The 5d←4f Excited States of $[Ce(OH_2)_9]^{3+}$. *Mol. Phys.* **1985**, *54*, 1293−1306.

(11) Kaizu, Y.; Miyakawa, K.; Okada, K.; Kobayashi, H.; Sumitani, M.; Yoshihara, K. Aqualigand Dissociation of $[Ce(OH_2)_9]^{3+}$ in the 5d←4f Excited State. *J. Am. Chem. Soc.* **1985**, *107*, 2622−2626.

(12) Miyakawa, K.; Kaizu, Y.; Kobayashi, H. An Electrostatic Approach to the Structure of Hydrated Lanthanoid Ions. $[M(H_2O)_9]^{3+}$ versus $[M(H_2O)_8]^{3+}$. *J. Chem. Soc., Faraday Trans. 1* **1988**, *84*, 1517−1529.

(13) Svetashev, A. G.; Tsvirko, M. P. Influence of Temperature on Spectral-Luminescent Properties of Trivalent Cerium Salts. *Theor. Exp. Chem.* **1985**, *20*, 653−658.

(14) Wang, J.; Mei, Y.; Tanner, P. A. Luminescence properties, Centroid Shift and Energy Transfer of Ce^{3+} in Aqueous Chloride Solutions. *J. Lumin.* **2014**, *146*, 440−444.

(15) Laurenezy, G.; Merbach, A. E. The Reaction Volume for the Equilibrium between the Lanthanide (III) Ennea- and Octaaqua Ions as a Diagnostic Aid for Their Water-Exchange Mechanisms. Preliminary Communication. *Helv. Chim. Acta* **1988**, *71*, 1971−1973.

(16) Helm, L.; Merbach, A. E. Inorganic and Bioinorganic Solvent Exchange Mechanisms. *Chem. Rev.* **2005**, *105*, 1923−1959.

(17) Kotzian, M.; Rösch, N. Electronic Structure of Hydrated Cerium(III). An INDO/S-CI Molecular Orbital Study Including Spin-Orbit Interaction. *J. Phys. Chem.* **1992**, *96*, 7288−7293.

(18) Andriessen, J.; van der Kolk, E.; Dorenbos, P. Lattice Relaxation Study of the 4f-5d Excitation of Ce^{3+}-Doped $LaCl_3$, $LaBr_3$, and $NaLaF_4$: Stokes Shift by Pseudo Jahn-Teller Effect. *Phys. Rev. B: Condens. Matter Mater. Phys.* **2007**, *76*, 075124.

DOI: 10.1021/acs.inorgchem.8b01224
Inorg. Chem. 2018, 57, 10111−10121

(19) (a) Albertsson, J.; Elding, I. The Geometry of the Nonaaqualanthanoid(3+) Complex in the Solid Bromates and Ethyl Sulphates. *Acta Crystallogr., Sect. B: Struct. Crystallogr. Cryst. Chem.* **1977**, *33*, 1460−1469. (b) Abbasi, A.; Lindqvist-Reis, P.; Eriksson, L.; Sandström, D.; Lidin, S.; Persson, I.; Sandström, M. Highly Hydrated Cations: Deficiency, Mobility, and Coordination of Water in Crystalline Nonahydrated Scandium(III), Yttrium(III), and Lanthanoid(III) Trifluoromethanesulfonates. *Chem. - Eur. J.* **2005**, *11*, 4065−4077. (c) Habenschuss, A.; Spedding, F. H. Di-μ-chloro-bis[heptaaqualanthanum(III)] Tetrachloride $[(H_2O)_7LaCl_2La(H_2O)_7]Cl_4$. *Cryst. Struct. Commun.* **1979**, *8*, 511−516. (d) Rogers, R. D.; Kurihara, L. K. f-Element/Crown Ether Complexes. 1. Synthesis and Structure of $[Y(OH_2)_8]Cl_3\cdot$(15-crown-5). *Inorg. Chim. Acta* **1986**, *116*, 171−177. (e) Bell, A. M. T.; Smith, A. J. Structure of Hexaaquadichloroyttrium(III) Chloride. *Acta Crystallogr., Sect. C: Cryst. Struct. Commun.* **1990**, *46*, 960−962.

(20) Shannon, R. D. Effective Ionic Radii and Systematic Studies of Interatomic Distances in Halides and Chaleogenides. *Acta Crystallogr., Sect. A: Cryst. Phys., Diffr., Theor. Gen. Crystallogr.* **1976**, *32*, 751−767.

(21) (a) Rogers, R. D. f-Element/Crown Ether Complexes. 26. Crystallization of Two Hydrated Forms of Hydrogen Bonded Complexes of $NdCl_3\cdot nH_2O$ and 15-crown-5. Crystal Structures of $[Nd(OH_2)_9]Cl_3\cdot$15-crown-5$\cdot H_2O$ and $[NdCl_2(OH_2)_6]Cl\cdot$15-crown-5. *Inorg. Chim. Acta* **1988**, *149*, 307−314. (b) Rogers, R. D.; Kurihara, L. K. f-Element/Crown Ether Complexes. 6.* Interaction of Hydrated Lanthanide Chlorides with 15-crown-5: Crystallization and Structures of $[M(OH_2)_8]C1_3\cdot$(15-crown-5) (M = Gd, Lu). *Inorg. Chim. Acta* **1987**, *130*, 131−137.

(22) Tapia, M. J.; Burrows, H. D.; Azenha, M. E. D. G.; Miguel, M. D.; Pais, A. A. C. C.; Sarraguca, J. M. G. Cation Association with Sodium Dodecyl Sulfate Micelles As Seen by Lanthanide Luminescence. *J. Phys. Chem. B* **2002**, *106*, 6966−6972.

(23) Frey, S. T.; Horrocks, W. D. Complexation, Luminescence, and Energy Transfer of Ce^{3+} with a Series of Multidentate Aminophosphonic Acids in Aqueous Solution. *Inorg. Chem.* **1991**, *30*, 1073−1079.

(24) (a) Choppin, G. R. Structure and Thermodynamics of Lanthanide and Actinide Complexes in Solution. *Pure Appl. Chem.* **1971**, *27*, 23−41. (b) Choppin, G. R.; Bertha, S. L. Lanthanide Complexation: Inner Versus Outer Sphere. *J. Inorg. Nucl. Chem.* **1973**, *35*, 1309−1312. (c) Choppin, G. R.; Unrein, P. J. Halide Complexes of the Lanthanide Elements. *J. Inorg. Nucl. Chem.* **1963**, *25*, 387−393. (d) Spedding, F. H.; Dekock, C. W.; Pepple, G. W.; Habenschuss, A. Heats of Dilution of Some Aqueous Rare Earth Electrolyte Solutions at 25 °C. 3. Rare Earth Chlorides. *J. Chem. Eng. Data* **1977**, *22*, 58−70. (e) Habenschuss, A.; Spedding, F. H. The Coordination (Hydration) of Rare Earth Ions in Aqueous Chloride Solutions from X-Ray Diffraction. I. $TbCl_3$, $DyCl_3$, $ErCl_3$, $TmCl_3$, and $LuCl_3$. *J. Chem. Phys.* **1979**, *70*, 2797−2806. (f) Habenschuss, A.; Spedding, F. H. The Coordination (Hydration) of Rare Earth Ions in Aqueous Chloride Solutions from X-Ray Diffraction. III. $SmCl_3$, $EuCl_3$, and Series Behavior. *J. Chem. Phys.* **1980**, *73*, 442−450.

(25) (a) Breen, P. J.; Horrocks, W. D. Europium(III) Luminescence Excitation Spectroscopy. Inner-Sphere Complexation of Europium(III) by Chloride, Thiocyanate, and Nitrate Ions. *Inorg. Chem.* **1983**, *22*, 536−540. (b) Rudolph, W. W.; Irmer, G. Raman Spectroscopic Characterization of Light Rare Earth Ions: La^{3+}, Ce^{3+}, Pr^{3+}, Nd^{3+} and Sm^{3+} Hydration and Ion Pair Formation. *Dalton Trans.* **2017**, *46*, 4235−4244.

(26) Kanno, H.; Hiraishi, J. Anomalous Concentration Dependence of the Inner-Sphere Hydration Number Change in Aqueous Europium(III) Chloride and Gadolinium Chloride Solutions. *J. Phys. Chem.* **1982**, *86*, 1488−1490.

(27) Kerridge, A. Quantification of f-Element Covalency Through Analysis of the Electron Density: Insights From Simulation. *Chem. Commun.* **2017**, *53*, 6685−6695.

(28) Zhang, J.; Heinz, N.; Dolg, M. Understanding Lanthanoid(III) Hydration Structure and Kinetics by Insights from Energies and Wave Functions. *Inorg. Chem.* **2014**, *53*, 7700−7708.

DOI: 10.1021/acs.inorgchem.8b01224
Inorg. Chem. 2018, 57, 10111−10121